

Status report and near future prospects for the gravitational wave detector AURIGA

J.-P. Zendri† §, L. Baggio‡, M. Bignotto||, M. Bonaldi§, M. Cerdonio||, L. Conti||, M. De Rosa ¶, P. Falferi§, P.L. Fortini⁺, M. Inguscio ¶, A. Marin||, F. Marin ¶, R. Mezzena‡, A. Ortolan*, G.A. Prodi‡, E. Rocco‡, F. Salemi⁺, G. Soranzo†, L. Taffarello†, G. Vedovato*, A. Vinante‡, S. Vitale‡

† Istituto Nazionale di Fisica Nucleare I.N.F.N., Sezione di Padova, Via Marzolo 8, I-35131, Padova, Italy.

‡ Department of Physics, University of Trento and I.N.F.N Gruppo Coll. di Trento Sezione di Padova, I-38050 Povo, Trento, Italy.

|| Department of Physics, University of Padova and I.N.F.N. Sezione di Padova, Via Marzolo 8, I-35131, Padova, Italy.

§ Centro CeFSA, ITC-CNR, Trento and I.N.F.N. Gruppo Coll. di Trento Sezione di Padova, I-38050 Povo, Trento.

*I.N.F.N. National Labs of Legnaro, Via Romea 4, I-35020 Legnaro, Padova, Italy.

⁺ Department of Physics, University of Ferrara and I.N.F.N. Sezione di Ferrara, I-44100 Ferrara, Italy.

¶ Department of Physics, University of Firenze and I.N.F.N. Sezione di Firenze, I-50125 Arcetri, Firenze, Italy.

Abstract. We describe the experimental efforts to set up the second AURIGA run. Thanks to the upgraded capacitive readout, fully characterized and optimized in a dedicated facility, we predict an improving of the detector sensitivity and bandwidth by at least one order of magnitude. In the second run AURIGA will also benefit from newly designed cryogenic mechanical suspensions and from the upgraded data acquisition and data analysis.

§ To whom correspondence should be addressed (zendri@lnl.infn.it)

1. Introduction

The first AURIGA run ended in November 1999 because of a cryogenic failure which imposed to warm-up the detector at room temperature. During the two years of data acquisition the detector reached the best strain sensitivity of $S_{hh}^{1/2} \approx 4 \cdot 10^{-22} \text{ Hz}^{-1/2}$ within a bandwidth of $\sim 2 \text{ Hz}$ around the two resonant frequencies (911 Hz and 929 Hz) [1] and duty cycle of $\sim 1/3$ of the total acquisition time. For an impulsive signal the AURIGA noise level corresponds to a minimal detectable Fourier transform amplitude of $H_0 \approx 2.5 \cdot 10^{-22} \text{ Hz}^{-1}$. Although the above sensitivity is among the best ever achieved, for the second AURIGA run we plan to use an upgraded readout optimized to widen the bandwidth to several tens of Hz . Thus we expect to increase the amplitude sensitivity of at least a factor ten.

To understand the pursued strategy let us model the resonant bar first longitudinal mode as an harmonic oscillator of equivalent mass M_{eff} and resonant frequency ω_b . An incoming gravitational wave of amplitude $h(t)$ drives the resonator with a force $F_{grav} \propto \ddot{h}(t)$ [2] and the induced oscillator displacement, which is the physical observable, contains all the information about the wave amplitude. The detector sensitivity is affected by at least two unavoidable displacement noise sources. The first comes from the amplifier stage and is described by two not completely correlated noise generators: *i*) the equivalent displacement noise generator x_n and *ii*) the back-action noise force generator F_{ba} which randomly drive the oscillator motion. The power spectrum of the back-action noise $S_{F_{ba}F_{ba}}$ and of the displacement noise $S_{x_nx_n}$ scales as α^2 and α^{-2} respectively [3], where α is the transduction efficiency, defined as the ratio between the displacement induced electrical signal measured at the amplifier input and the mechanical oscillator motion amplitude. According to quantum mechanics predictions none of these two noise power spectra can vanish as they must satisfy the inequality $S_{F_{ba}F_{ba}}^{1/2} \cdot S_{x_nx_n}^{1/2} \geq \hbar/2$ [4]. In practice real amplifiers operate $N_{\hbar} \sim 10^2 \div 10^4$ times above this level. Thus in order to improve the sensitivity the first requirement for a readout is to employ amplifiers which operate as close as possible to the quantum limiting value $N_{\hbar} = 1$. The best value achieved for the first AURIGA run using a commercial dc-SQUID as the first amplification stage was $N_{\hbar} \approx 4000$ while as discussed below for the second run we will employ a two-stage SQUID amplifier which approaches $N_{\hbar} \approx 100$.

The second unavoidable noise source affecting the detector sensitivity is the thermal noise which is described by the Langevin force F_{Th} with power spectrum $S_{F_{Th}F_{Th}} = 2k_B T M_{eff} \omega_b / Q_b$, where k_B is the Boltzmann constant, Q_b is the harmonic oscillator quality factor and T its temperature. Both back-action and Langevin noise sources act on the mechanical resonator as disturbance forces that limit the sensitivity to the gravitational force F_{grav} . To include all the noise sources in the sensitivity analysis we define the equivalent displacement noise force generator F_{n-eq} as the noise force generator which produces at the output port the measured displacement noise x_n . Thus the force generator noise power spectrum is defined as $S_{F_{n-eq}F_{n-eq}} = S_{x_nx_n} / |G(\omega)|^2$, where $G(\omega) = M_{eq}^{-1}(\omega_b^2 - \omega^2 + i\omega_b\omega/Q_b)^{-1}$ is the transfer function of the oscillator

force. In figure 1 the power spectrum of the noise forces are plotted; the total noise curve which is the sum of all components is also shown. Figure 1 shows that in general any increase of the transduction efficiency α is accompanied by an increase of both the bandwidth and the sensitivity: the lower level of the total noise curve is dominated by the α -independent thermal noise contribution while $S_{F_{n-eq}F_{n-eq}}$ decreases as α^{-2} . When the transduction efficiency becomes very high the minimum of the total noise curve is dominated by the back-action contribution and therefore it scales as α^2 . At this point any further increase of α correspond to widen the detector bandwidth without improving its sensitivity. However, as this limit condition is far from being achieved [3], we have to maximize the transduction efficiency in order to optimize the readout.

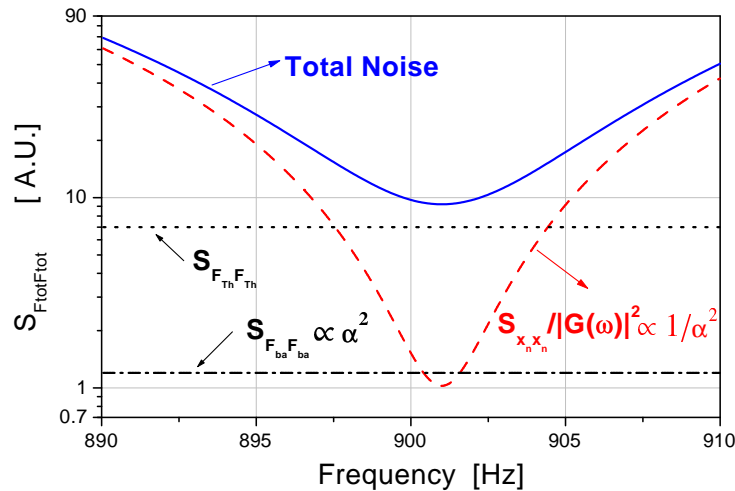


Figure 1. Power spectrum of the the noise forces acting on the single-mode resonant detector. The dashed line, which scales as α^{-2} , is the contribution coming from the amplifier broad band displacement noise, the dotted line the thermal noise contribution and the dot-dashed line the back-action contribution, which scale as α^2 . The overall noise curve (filled line), which is the sum of all the above components, is also plotted.

In section 2.1 we describe our efforts to meet the above requirements (minimization of N_h and maximization of α) and the state of the art. Section 2.2 is devoted to the description of the new cryogenic suspension developed to fully exploit the bandwidth increase and section 2.3 to the upgrades of the detector cryogenics. In section 2.4 we report the expected sensitivity for the second run. Finally in section 2.5 we outline the new features of the data acquisition and analysis.

2. The second Auriga run

2.1. Transduction and amplification

In the second run the AURIGA detector will be equipped with a resonant capacitive transducer read by a two-stage SQUID amplifier. To maximize the signal transfer from

the transducer output to the SQUID input coil, a high turn ratio superconducting transformer is inserted between them. The transducer capacitance C and the transformer primary coil form an electrical resonator with resonant frequency $\omega_{el} = (L_{eff}C)^{-1/2}$, where $L_{eff} = L(1 - k^2L_s/(L_s + L_{in}))$, $k^2 = M^2/(LL_s)$ is the transformer geometrical coupling, M the transformer mutual inductance, L_{in} the SQUID input coil self-inductance, L and L_s respectively the primary and the secondary coil inductance of the transformer. For this experimental set-up and assuming that the electrical resonant frequency is far from the mechanical resonant frequencies ω_{mec} the frequency dependent transducer efficiency α_{Cap} becomes approximately:

$$\alpha_{Cap} = \frac{ME_0\omega}{L_{eff}(L_s + L_{in})} \frac{1}{\omega_{el}^2 - \omega^2 + i\omega_{el}\omega/Q_{el}} \left[\frac{A}{m} \right] \quad (1)$$

where E_0 is the transducer electric bias field and Q_{el} the electric resonator quality factor. When $\omega_{el} \gg \omega_{mec}$, as in the first AURIGA run, the above formula, for the optimal condition $L_{in} \approx L_s$, takes the simple form $\alpha_{Cap} = E_0\omega k C^{1/2}/(2\omega_{el}^2\sqrt{L_{in}})$ which states that, given any electrical resonance ω_{el} , the way to maximize the transduction efficiency is to maximize the transducer bias field and capacitance and the transformer geometrical coupling k . An improvement of at least one order of magnitude on both the first two parameters is the main goal of the present research and development program on the capacitive transducer. However, as this program is still work in progress, the second AURIGA run will employ an alternative method to maximize α . Indeed, as suggested by equation (1), by equating the electrical mode resonant frequency to the mechanical one a huge increase of the transduction efficiency is expected around the frequencies where the gravitational wave induced displacement is largest. The soundness of this procedure becomes evident in figure(2) where the calculated detector bandwidth is plotted for different values of ω_{el} and reaches its maximum value when the mechanical and the electrical modes are tuned. The drawback of this procedure is that it requires very high electrical quality factor ($Q_{el} \approx 10^6$) to preserve high sensitivity and strong rejection of electromagnetic interferences. To this aim the superconducting transformer is assembled with intrinsically low-loss dielectric materials and housed in a superconducting box designed by finite element methods (FEM) to avoid spurious mechanical resonances in the frequency range of interest.

Even with the predicted improvement of the transduction efficiency the transducer for the next AURIGA run will still be resonant with the bar oscillator. However, as a consequence of the increment of α , less mechanical amplification is required and thus the transducer resonant plate can be made heavier with a consequent bandwidth improvement. Indeed the optimal transducer mass is now [5] about 4 kg, 10 times bigger than the one used in the previous run. The new transducer was designed using FEM to avoid spurious resonances and to keep the internal-stress gradient as low as possible (in order to reduce thermoelastic losses). Basically it has the usual mushroom geometry [6], with the central part of the membrane thinned to match the requirement of high mass and resonant frequency tuned to the the bar one (≈ 900 Hz).

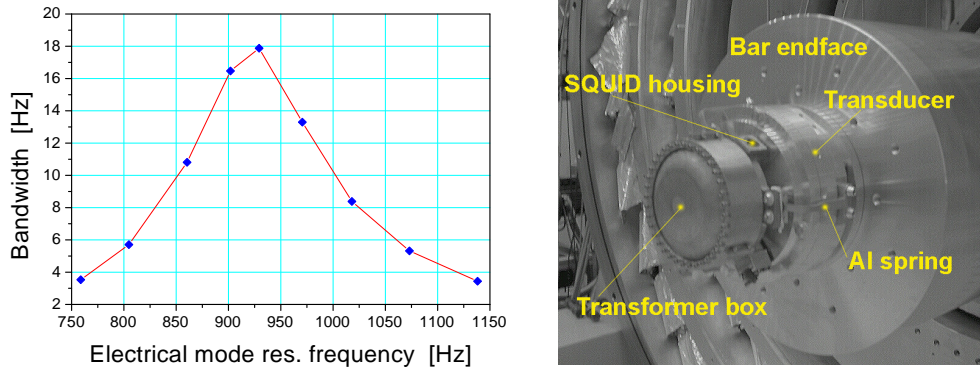


Figure 2. Left: The overall detector bandwidth calculated for different electrical resonance frequencies. The mechanical resonance is at 920 Hz while the used amplifier is a single dc-SQUID. Right: Picture of the new transduction line connected to the bar end-face. It is possible to see the capacitive transducer which through an Aluminum spring is mechanically connected to the superconducting box (a deposition of Sn-Pd over a copper core) which contain both the superconducting matching transformer and the two SQUIDs.

The second requirement for an optimal transduction chain is to incorporate an amplifier stage operating near the quantum limited energy sensitivity ($N_{\hbar} = 1$). In principle in our frequency range a SQUID amplifier can approach this limit. However, the noise level of the single SQUID amplifier is strongly affected by the room temperature electronic which adds a temperature-independent noise contribution. In order to overcome this problem we developed a two-stage SQUID in which the sensor SQUID voltage output is amplified by a second low noise SQUID. This two stage SQUID demonstrated to work in the temperature range between 4.2 K and 50 mK with a broadband noise power spectrum which scales linearly with the thermodynamic temperature, as expected for intrinsic noise limited SQUID, down to 300mK [7]. When coupled to an high quality factor electrical resonator the measured energy sensitivity of the device at 4.2 K was about $N_{\hbar} = 420$, linearly decreasing with temperature to $N_{\hbar} = 200$ at 1.5 K [8]. The energy sensitivity at lower temperature has still to be investigated. As the two-stage SQUID is based on a commercial device with the input coil strongly coupled to the SQUID loop, it is particularly suitable for the integration in a high sensitive transducer chain and thus will be employed in the second AURIGA run.

The massive transducer, coupled to the high Q transformer and read by the two-stage SQUID amplifier, was tested in the transducer test facility within the temperature range $1.6 \div 4.2$ K. The detailed results of these measurements are described elsewhere [9]. Let us just remark here that the tested transduction chain, assembled as it will operate in the AURIGA detector, operated with an amplifier energy resolution ($N_{\hbar} = 350$ at 1.6 K) not too far from the SQUID noise level measured in bench tests. The measured electrical quality factor, $Q_{el} = 10^6$, the absence of any measurable electromagnetic interference

contribution and the obtained high geometrical coupling $k = 0.86$ meet the requirements. Finally differently from the previous run, the superconducting transformer and the SQUIDS housing box are placed close to the transducer (see fig.2) with the aim of reducing microphonicity noise. Thanks to the softness of the connection, given by Al springs, this operation does not affect the transducer mechanical quality factor, which at cryogenic temperature turns out to be $Q_t = 1.4 \cdot 10^6$.

2.2. Suspensions

To exploit the predicted sensitivity and bandwidth improvement, in the second run AURIGA will be equipped with a new cryogenic suspension, optimized for broadband operation. The main mechanical filter is a cascade of six “spring-mass” elements forming together a column of 25 cm diameter and 80 cm length (total mass 130 kg). Each spring element, which at 1kHz should provide an attenuation of -40 dB, is designed to operate with a static internal stress less than 25% of the yield stress of the material (the high strength aluminum alloy “Alumold 1-500”). Basically it is composed by three “C” shaped elements machined in a single piece in a “trefoil” configuration, which provides a good attenuation in all the six degrees of freedom. The brass masses of the single suspension element are bolted to the spring monolithic piece. According to the FEM prediction, the vertical resonant frequency should be 95 Hz while no other internal resonances should appear in the frequency window $200 \div 1800$ Hz. The assembling of the new suspensions and their connections to the old AURIGA cryostat are described in figure 3.

Another interesting feature of the new suspension system is the bar hanging method. Instead of the old belly cable around the bar middle section, the bar will hang from its center of mass by a tubular cable. The tubular geometry has been chosen in order to maintain the longitudinal mechanical attenuation while avoiding the presence of the violin modes in the frequency range of interest. The expected advantages of this procedure are an improvement of attenuation and of the bar quality factor as a consequence of the lower coupling between the bar longitudinal mode and the suspension motion [10].

The simulation by finite elements modeling software predicts an overall attenuation of 300 dB at 1kHz without any expected internal resonance in the frequency window between 700 and 1200 Hz. At the moment of writing almost all the new suspension parts have been delivered and tests are being performed.

2.3. Cryogenics

As expected, the ultracryogenic detectors achieved a better sensitivity levels with respect to warmer resonant detectors. However, this advantage was achieved at the cost of a decreased duty cycle [11]. This is due to worse reliability in the operation of the ^3He - ^4He dilution refrigerator. In addition the refrigerator 1K-pot has been demonstrated to be a source of mechanical disturbance, making blind the detector during the daily

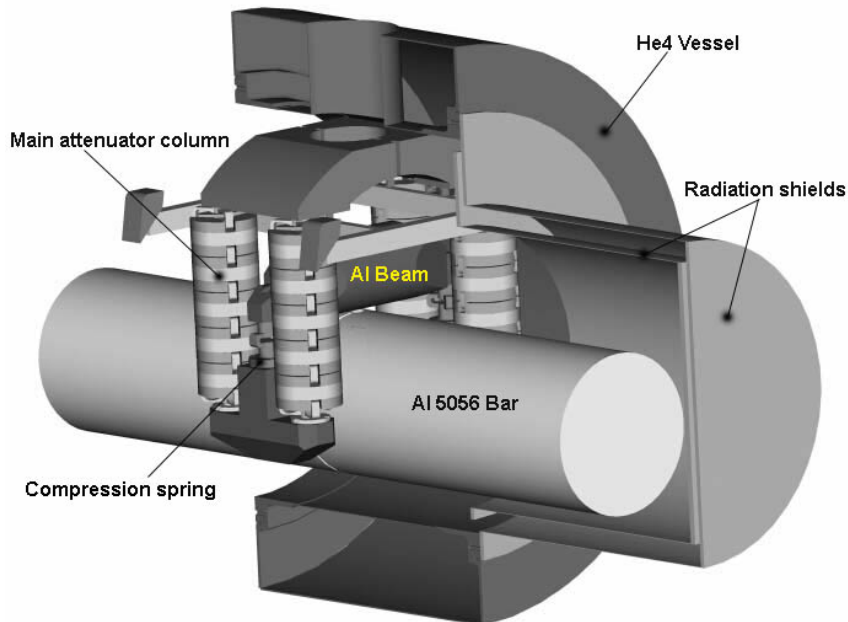


Figure 3. Cross section of the new AURIGA cryogenic suspensions. The 4K vessel of the cryostat supports a stainless steel frame, to which the whole suspension system is hung. The four main suspension columns are fixed to a big 300 kg “D-shaped” aluminum mass, supported by four titanium springs. The aim of these four spring is to uncouple the steel frame from the columns. Each pair of columns supports an inverted “T” aluminum mass on the top of which is fixed a compression spring with an upper conical joint which is used to lean an aluminum beam. The bar hangs at its center of mass with a tubular cable which is attached with a “bayonet” mount into the aluminum beam. The insertion point into the antenna has been designed with a conical surface of joint at an angle of 45° . The contact area of the two surfaces guarantees a good thermal link for the antenna.

refill. Given this we decide to split the second AURIGA run in two phases. During the first one the dilution refrigerator will be substituted by a ^4He pumped dewar with a capability of about 150 liters. This operation is expected to achieve a stable cryogenic point at 1.5 K. In the second phase, a modified dilution refrigerator will be added to reach the lowest temperatures. In particular, a new 1K-pot is being designed using FEM analysis to avoid any internal resonance in the kHz frequency region. Furthermore, the new 1K-pot will incorporate the recently developed recipes to avoid its vibrational noise ‡.

2.4. Expected Sensitivity

In table 1 we report the main dynamic parameters used for the calculation of the sensitivity for the second AURIGA run. The transducer and the electronic readout parameters as well as the values of the two SQUID noise power spectrum are those actually measured in the transducer test facility. The bar parameters are the same

‡ A. Raccanelli, Max Plank Institute für Radioastronomie, Bonn (D), private communication

obtained in the previous run except for the bar resonant frequency which is lowered by the presence of a more massive transducer basement[†].

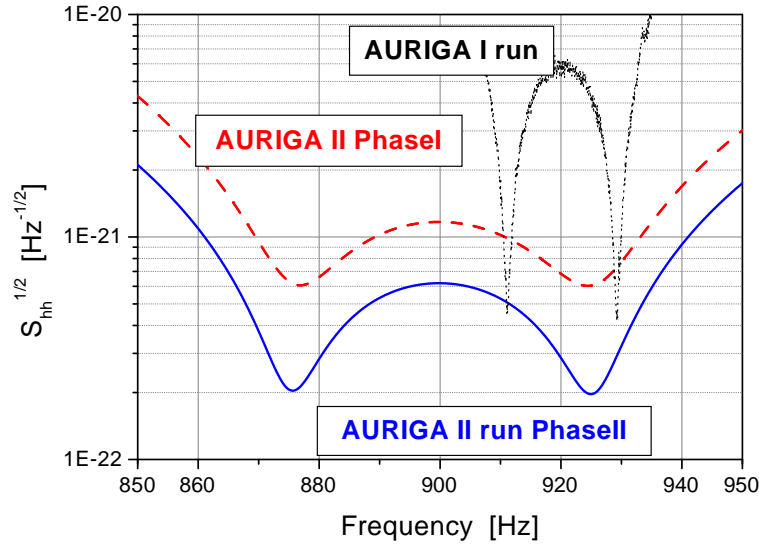


Figure 4. The predicted sensitivity curve for the second AURIGA run. The dashed line correspond to the first phase with the detector operating at 1.5 K, the filled line the detector operating at 0.1 K. For comparison is also reported (dotted line) the sensitivity obtained for the first AURIGA run

The sensitivity curves expected for the two phases of the second run are plotted in fig(4); for comparison the sensitivity measured in the previous AURIGA run is also plotted. They can be used to calculate the pulse Fourier amplitude H_{min} at $S/N=1$. For the first phase we get $H_{min} = 6 \cdot 10^{-23} \text{ Hz}^{-1}$, which correspond to a bar absorbed energy E_{min} five times bigger than the minimum achievable [13] using a $N_h = 350$ SQUID amplifier (as our two-stage SQUID at 1.5 K). This result suggests that although we have optimized the transduction chain the thermal noise is still very important.

This situation is better, but still not optimized, is the situation for the phase II in which the predicted minimal detectable amplitude of $H_{min} = 2.5 \cdot 10^{-23} \text{ Hz}^{-1}$ corresponds to an energy resolution of about $250 \hbar \omega_b$, more than two times the minimum achievable. However differently for of the phase I curve, which was predicted using already measured parameters, the phase II curve is drawn using a SQUID back-action power spectrum value which is the extrapolation at 0.1 K of that measured in the temperature range $1.5 \div 4.2$ K. The measurements of the SQUID noise properties at ultracryogenic temperature will be performed in the near future.

Finally a sensitivity improvement should be obtained reducing the thermal noise level, for instance increasing the bar quality factor, or reducing its effect through the

[†] We calculate the expected resonant frequency according to the empiric formula [12] which states that any mass connected to the bar endface reduces the resonant frequency of about 0.3 Hz/kg. However the real value will be soon estimated measuring, at room temperature, the frequencies of the transducer-bar two modes system.

Table 1. Table of the relevant parameters used for the calculation of the sensitivity curve of fig.4. The parameters values come from the measurements in the transducer test facility or from the previous AURIGA run.

<i>Parameter</i>	<i>Symbol</i>	<i>Value</i>
Bar Mass	m_b	2230 kg
Bar Length	L_b	2.93 m
Bar Resonant Frequency	$\nu_b = \omega_b/2\pi$	902 Hz
Bar Quality Factor	Q_b	$8 \cdot 10^6$
Transducer mass	m_t	4.0 kg
Transducer resonant frequency	$\nu_t = \omega_t/2\pi$	909 Hz
Transducer Quality Factor	Q_t	$1.5 \cdot 10^6$
Transducer bias field	E_0	10^7 V/m
Primary Coil Inductance	L	6.5 H
Secondary Coil Inductance	L_s	3.2μ H
Transformer Mutual Inductance	M	3.8 mH
SQUID input coil	L_{in}	1.8μ H
SQUID mutual inductance	M_{sq}	10 nH
Electrical Quality factor	Q_{el}	10^6

increase of the transduction efficiency. Both these advantages should be obtained already during the phase I of the run thanks to the new design of the mechanical suspensions and to the incremented transducer bias field.

2.5. Data acquisition and data analysis

The data acquisition and data analysis systems has been fully redesigned and upgraded to satisfy the new requirements of the second AURIGA run (wider bandwidth and higher sensitivity) and allow to the operation of AURIGA in an intercontinental network of bar and interferometric gw detectors [14]. To this goal, we have adopted the FRAME format (developed by VIRGO/LIGO) for the Input/Output and for future data exchange. The PC Linux, the open source tools and libraries and the C++ programming language have been the natural choice for the development platform. We have developed two libraries: i) the Process Control Library (PCL) aimed to manage communications and controls of the user processes, and ii) the AURIGA Algorithm Library (AAL) which gathers the specific algorithms of the AURIGA analysis (adaptive filters, template matching, trigger extraction). The AAL Library addresses also the problems of unbiased estimation of signal parameters and the setup of the data quality and data validation procedures. We are also developing an interactive tool of data analysis based on CINT/ROOT for data monitor and diagnostic purposes.

3. Conclusions

Within few months the AURIGA detector will start its second acquisition run. Thanks to the up-graded transduction chain, already tested on the test facility, an improvement

of about a factor ten in amplitude sensitivity is expected. In terms of energy resolution this correspond to only few hundred times the fundamental standard quantum limit. An attempt to increase the duty cycle and to understand the origin of the non-stationary noise will be made by splitting the second run in two different phases. During the first phase the detector will operate at 1.5 K, which should favour a stable and quiet cryogenic condition. In the second phase the detector will operate at ultracryogenic temperature, using an upgraded dilution refrigerator optimized for long term and quiet operation. Finally an improvement both on sensitivity and duty cycle is expected from the use of the new suspensions optimized for broadband operation. The upgraded AURIGA detector with the new data analysis will be also ready to join the interferometric network of gravitational wave detectors.

References

- [1] J.P. Zendri *et al.*, in: *Gravitational waves*, proc. of the ‘Third E. Amaldi Conference’, (CalTech - California, 1999), ed. by S.Meshkov, AIP Conf. Proc., New York (2000) p. 421.
- [2] See for instance C.W. Misner, K.S. Thorne and J.A. Wheeler, *Gravitation* W.H. Freeman and company, New York, 1973
- [3] J.P. Zendri *et al.*, in *Recent Developments in General Relativity*, proc. of the XIV Congress on General Relativity, (Genova, Italy, Sept. 2000), Springer-Verlag p.285-299 in press.
- [4] C.M. Caves, *Phys. Rev.* **D26**, 1817 (1982).
- [5] V. Crivelli Visconti, *PhD thesis*, University of Padova, available at <http://www.auriga.inl.infn.it>.
- [6] P. Rapagnani *Il Nuovo Cimento* **5C**, 385 (1982).
- [7] R. Mezzena *et al.*, A. R. Mezzena *et al.*, *Rev. Sci. Instrum.* **72**, 3694 (2001).
- [8] A. Vinante *et al.*, in these proceedings.
- [9] A. Marin *et al.*, in these proceedings.
- [10] E. Coccia, *Rev. Sci. Instr.* **55**, 1980 (1984).
- [11] G.A.Prodi *et al.*, in these proceedings.
- [12] S. Paoli, graduate thesis, University of Padova.
- [13] J.C. Price, *Phys. Rev.* **D36**, 3555 (1987).
- [14] A. Ortolan *et al.*, in these proceedings.